Manufacturing of a porous metallic panel by spark plasma sintering for hybrid laminar flow control application

Baptiste Egreteau, Cécile Davoine, Fabien Méry, Olivier Vermeersch, Marc Thomas

Manufacturing Of a Porous Metallic Panel by Spark Plasma Sintering For Hybrid Laminar Flow Control Application

Baptiste Egreteau[1] baptiste.egreteau@onera.fr; Cécile Davoine[1] cecile.davoine@onera.fr; Fabien Méry[2] fabien.mery@onera.fr; Olivier Vermeersch[2] olivier.vermeersch@onera.fr; Marc Thomas[1] marc.thomas@onera.fr

[1] DMAS, ONERA, Paris Saclay University, F-92320 Châtillon, France
[2] DMPE, ONERA, Toulouse University, F-31055 Toulouse, France

Abstract

Hybrid laminar flow control uses wall suction through a porous panel to delay the so-called laminar-turbulent transition, thus reducing the aircraft fuel consumption. This technology requires a skin panel with very good transverse permeability and an excellent surface finish. Currently, laser micro-perforated titanium panels are used, but the minimum diameter of the holes is limited, hindering a better suction distribution. Moreover, these titanium panels are difficult and expensive to produce. This is the reason why spark plasma sintering is used here to produce a porous material through partial densification of Ti64 powder. The samples have been characterised through tomography, and permeability tests to correlate the material's structure with its suction performances. Indeed, as spark plasma sintering is a field assisted manufacturing process, the material might have enhanced suction performance in the application direction of the electric field.

Main text

1. Introduction

Hybrid laminar flow control (HLFC) is a technology, which aims at reducing aircrafts fuel consumption. It acts on the boundary layer that develops on the aircraft's surfaces. This boundary layer can be either laminar with a smooth flow, or turbulent with a chaotic flow. What is important is that skin friction is 5 to 7 times higher with a turbulent boundary layer compared with a laminar one. Thus, by applying suction through the surface, which the boundary layer is developing on, the laminar region can be extended. This extension of the laminar region induces an overall drag decrease and then a fuel consumption reduction. The concept of this system is synthesized in Figure 1

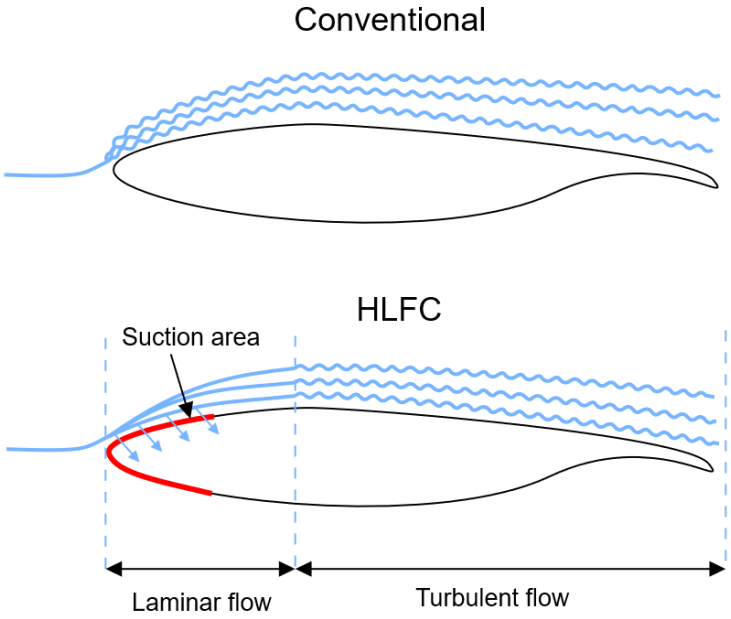

Figure 1: Concept of the HLFC system

This technology has already been employed on the tail of the Boeing 787 [1]. In this particular case, the suction is applied through a laser micro drilled titanium sheet. However, the manufacturing of these panels is difficult because the perforations need to be made after the shaping of the sheets. Moreover, the control of the holes shape and diameter is hard to maintain with their small diameter

(around 100 µm). With the new manufacturing techniques based on powder metallurgy, it seems possible to make porous panels through which suction could be applied. For example, a sintered 316L steel panel has already been tested in wind tunnel and proved to be at least as performant as classical perforated titanium sheets [2].

Many manufacturing techniques based on powder metallurgy are available. They could be categorised in three kinds. First, the fusion based techniques, such as laser powder bed fusion (LPBF) for which a high-energy laser beam melts locally powder to make parts layer by layer. This technique starts to be widely used in the industry and gives a good control on the materials shape, but it is still difficult to make well-controlled small size percolating porous networks [3]. Second, the plastic deformation based techniques, such as cold spray. In this case, powder is blown out at high speed so that the impact energy plasticizes the powder particles to make them integral with the substrate. In such a way, this is not easy to control the regularity of the samples thickness. Finally, there are sintering based techniques, such as hot isostatic press (HIP) or spark plasma sintering (SPS). There, powder particles are consolidated by applying a high temperature and/or a high pressure without having any liquid phase. There is only solid diffusion occurring at the contact point between the particles. SPS is the manufacturing process that we have chosen to work with. A sketch of SPS can be seen in Figure 2.

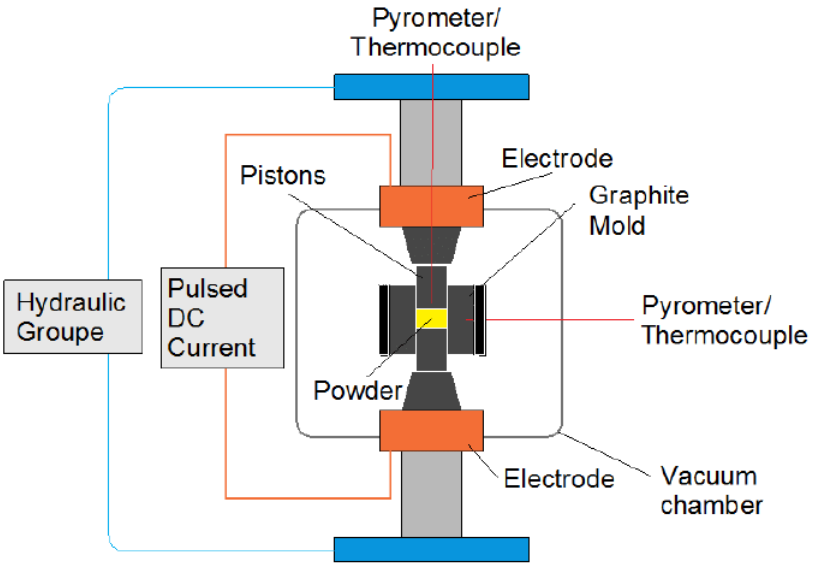

Figure 2 : Schematic of SPS manufacturing processes [4]

2. The manufacturing process: spark plasma sintering

Spark plasma sintering allows powder sintering very rapidly by applying high temperature and pressure. Metal powder is loaded in a cylindrical graphite die sealed with conductive carbon paper. This die is placed in a hydraulic press with graphite pistons so that high pressure and electric current can be applied at the same time. The current passing through the die and the powder induces a temperature increase due to the Joule effect. This temperature can be controlled with a thermocouple placed inside the die. When operating a SPS facility, a set of 4 parameters has to be monitored:

- The heating rate (usually 100°C/min)
- The temperature (up to 2500°C)
- The pressure (up to 1 GPa)
- The time during which temperature and pressure are maintained

The effect of these parameters is displayed in Figure 3.

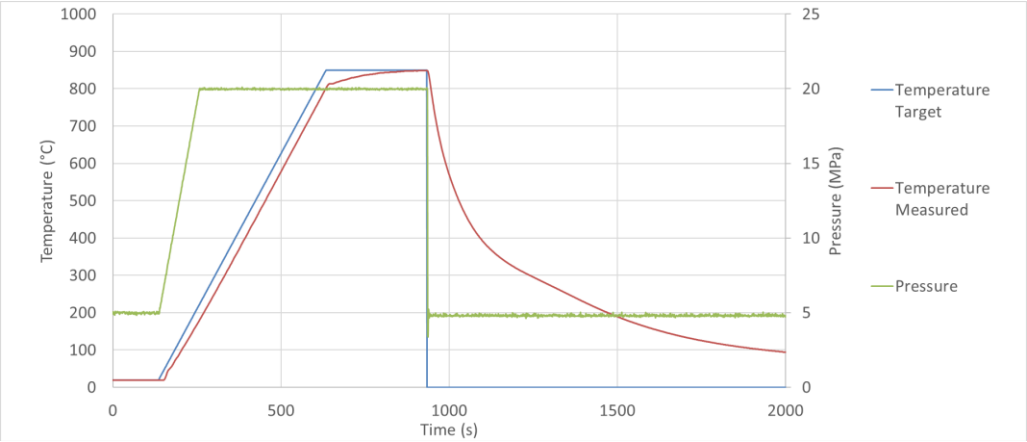

Figure 3: Time evolution of pressure and temperature of a SPS experiment

Initially, this technique was supposed to sinter powders of ultra-high temperature materials with very low porosity rates in short time (a few minutes) compared to several hours for HIPing. Nevertheless, its use can be diverted to create porous metallic samples [5]. The internal porous network structure could even be controlled. The most practical way is to sinter at lower conditions of pressure and temperature, resulting in a partial powder densification. The resulting pores morphology should then depend on the sintering parameters (temperature, pressure, duration) and the powder characteristics (particle size and shape). Moreover, as the pressure and electric current are applied only in the transversal direction, the porous network can be expected to be anisotropic with a preferred direction through the thickness of the panel, which is exactly what is required for the HLFC application.

Other strategies can be used such as spaceholders. Here, the metal is mixed with another powder that can be made of various materials (salt, ammonium bicarbonate, another metal …). The mixture is then sintered by taking care that the spaceholder does not collapse nor diffuse into the metal. Then, either the space holder decomposed under the temperature effect, either a dissolution step is required to obtain the porous material.

3. Experimental Procedures

The purpose of the following tests is to study the influence of the SPS operating parameters on the porous network inside the outcoming samples. For these experiments, gas atomised spherical Ti-64 powder with diameters ranging from 200 to 250 µm has been used. Large diameter powder particles were preferred to more classical finer powder (around 50µm diameter) to have large enough pore space between powder particles, thus ensuring the porous network to percolate. Only the influence of sintering temperature and pressure will be studied here. Sintering parameters were chosen from the work of Yamanoglu et al. [6] made on another titanium alloy, as gathered in

Temperature (°C) / **Pressure (MPa)**	**750**	**800**	**850**
5	T3P2	T2P2	T1P2
20	T3P1	T2P1	T1P1

Table 1. It resulted in 3 levels of temperature (750, 800, 850°C) and 2 of pressure (5 and 20 MPa). The 6 samples were made of 15g of powder in 36 mm diameter dies sintered during 5 minutes. After manufacturing, the carbon paper layer sticking to the samples has been removed with a coarse polishing. The result can be seen in Figure 4 where the dark spots on the sample after polishing are surface porosities in which there might be carbon debris that were removed in an ultrasonic bath.

Temperature (°C) / **Pressure (MPa)**	**750**	**800**	**850**
5	T3P2	T2P2	T1P2
20	T3P1	T2P1	T1P1

Table 1 : Identification of the samples depending on the sintering parameters

Figure 4: Sample before (left) and after (right) first coarse polishing

4. Material Characterisation

The HLFC application requires the suction panel to have good surface quality and suction performance. These characteristics will be analysed here and related to the internal porous network structure.

a) Surface Quality

From an aerodynamic point of view, surface defects may cause early transition by speeding up the destabilisation of the laminar boundary layer [7]. This is why classical titanium sheet for HLFC application have an average roughness of about 1µm. The porous material should reach this target. To do so, polishing has been carried out. After a first coarse polishing that removed the carbon paper, a finer one was done with a P600 paper. This operation gave a better surface finish and opened more widely the porosities at the surface as illustrated in Figure 5.

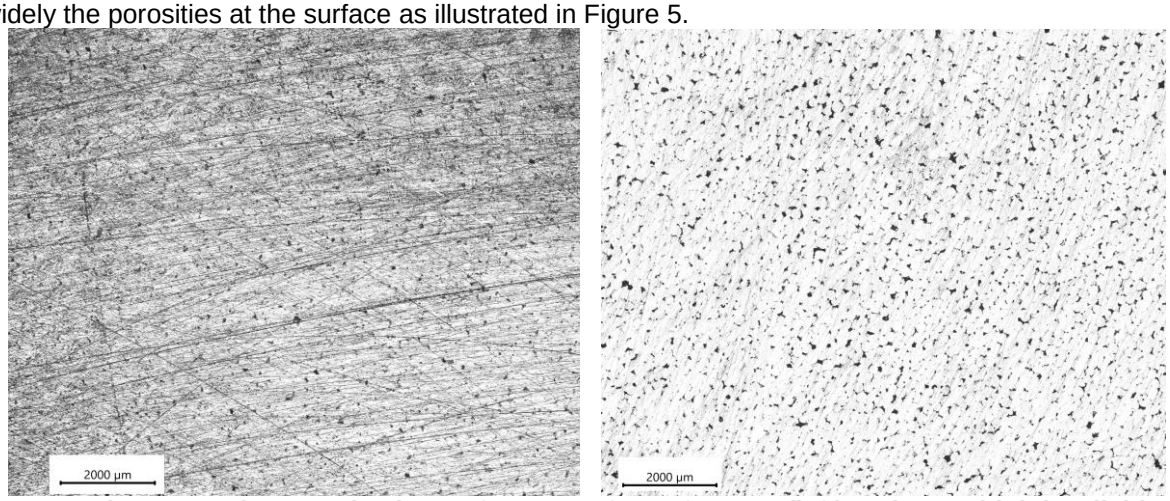

Figure 5 : Microscopic views of T1P1 surface after P80 (left) and P600 (right) polishing paper

It is very important to keep surface porosities as much open as possible, otherwise the suction performance of evaluated later will not be representative for the material porous network structure. This is why finer polishings were done after removing the carbon layer. Indeed, coarse polishing papers efficiently remove material but with the detrimental effect of surface plastic deformation that tends to clog the porous network.

After the surface finish, the average roughness of the samples has been evaluated with an optical profilometer (Bruker alicona InfiniteFocusSL). The results are gathered in

Sample	**T1P1**	**T1P2**	**T2P1**	**T2P2**	**T3P1**	**T3P2**
Average Roughness *Sa* [µm]	0.8	1.6	1.8	4.7	2.6	4.1
Standard Deviation *σ* [µm]	2.4	4.5	5.3	11.7	6.5	9.8
Maximum Peak Height Sp [µm]	51.8	19.0	32.1	23.4	21.6	16.2
Maximum Valley Depth Sv [µm]	67.3	105	109	168	118	135

Table 2.

Sample	**T1P1**	**T1P2**	**T2P1**	**T2P2**	**T3P1**	**T3P2**

Average Roughness *Sa* [µm]	0.8	1.6	1.8	4.7	2.6	4.1
Standard Deviation σ [µm]	2.4	4.5	5.3	11.7	6.5	9.8
Maximum Peak Height Sp [µm]	51.8	19.0	32.1	23.4	21.6	16.2
Maximum Valley Depth Sv [µm]	67.3	105	109	168	118	135

Table 2 : Profilometer results

Polishing with a P600 paper gave a satisfying average roughness for all samples with values below 5µm. To go further, it can be seen that the more the sintering temperature and pressure are decreased, the more the roughness is increased. We can relate this trend to the porosity ratio. Indeed, the less the powder is sintered, the more the porosity ratio is increased which leads to have more negative defects at the surface that are the inlet of the porous network. This is confirmed by the fact that the maximum valley depths are one order of magnitude greater than the maximum peak heights for all samples except the most sintered. This leads to artificially degrade average roughness and standard deviation.

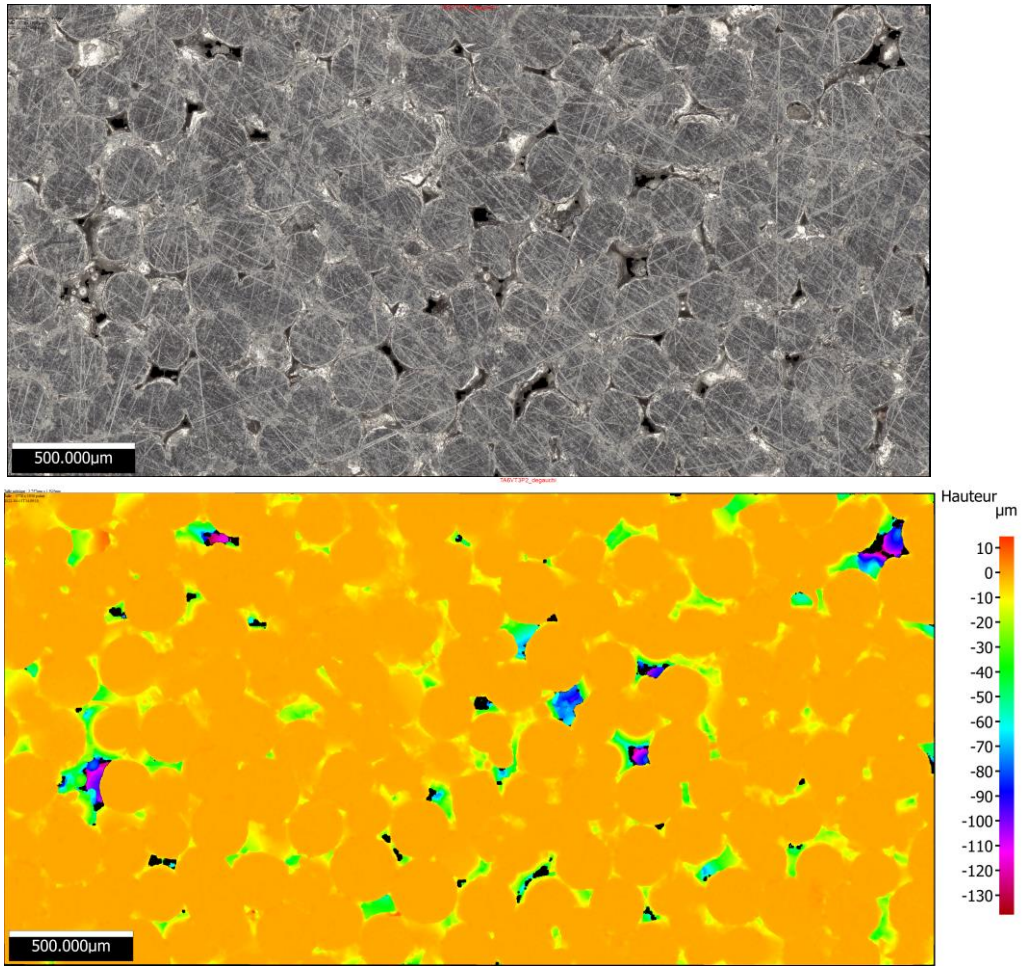

Figure 6 : Heights maps for T3P2 sample (bottom) and associated view (top)

Moreover, as shown in Figure 6, powder particles are approximately all at the same height with little valleys between them. These valleys may have two origins. Either the contact point between particles stands in this place slightly below the reference plane, or the polish is not fine enough. This means there is still plastic deformation obstructing the porous network. In order to avoid this problem, finer polishing has been conducted (P1200 and P2400 papers). It could only improve the surface quality, which was already satisfying. Polishing with P4000 paper has been made on T1P1 and T3P2 to see if it was relevant to refine further polishing, but it did not seem to open more the biggest porosities, which are the most important for a good flow.

b) Permeability Tests

Once the samples have an acceptable surface quality, their permeability needs to be evaluated. Permeability is the capacity of a porous material to allow fluids to pass through it. Darcy Forchheimer law models it (Equation 1):

$$-\nabla P = \frac{\mu}{K} V + \rho \beta V^2$$

Equation 1: Darcy-Forchheimer law

With:

- ∇P [Pa m^{-1}]: Pressure gradient through the porous medium
- μ [kg m^{-1} s^{-1}]: Fluid dynamic viscosity
- ρ [kg m^{-3}]: Fluid specific mass
- V [m s^{-1}]: Mean velocity in the porous media
- K [m^2] : Darcy coefficient associated to viscous permeability
- β [m^{-1}] : Forchheimer coefficient associated to inertial permeability

By determining both Darcy and Forchheimer coefficients, the pressure losses through the samples are fully characterised. To do so, the experimental set up sketched in Figure 7 has been used. The idea here is to induce an air mass flow rate which, knowing the temperature and the injection diameter, gives the velocity, and then to measure, in the stationary state, the pressure difference between the plenum and the exit. Then, knowing the sample thickness, the pressure gradient can be computed. After doing such measurements for different injection mass flow rates, a quadratic regression between the pressure gradient and the injection velocity is made to deduce Darcy and Forchheimer coefficients.

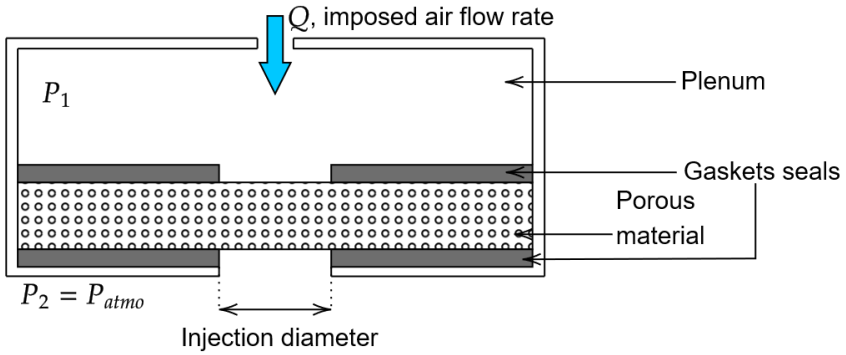

Figure 7 : Sketch of the permeability test bench

These measurements were made on six samples and it appeared that the relationship between the pressure gradient and the injection velocity was always linear. This means that the flow was viscous and then it was not relevant to compute the Forchheimer coefficient. This is why, only the Darcy coefficient is studied here.

Sample	T1P1	T1P2	T2P1	T2P2	T3P1	T3P2
Darcy coefficient [m^2]	9.12E-14	1.96E-13	5.74E-13	3.39E-12	1.69E-12	9.82E-12

Table 3: Darcy coefficients

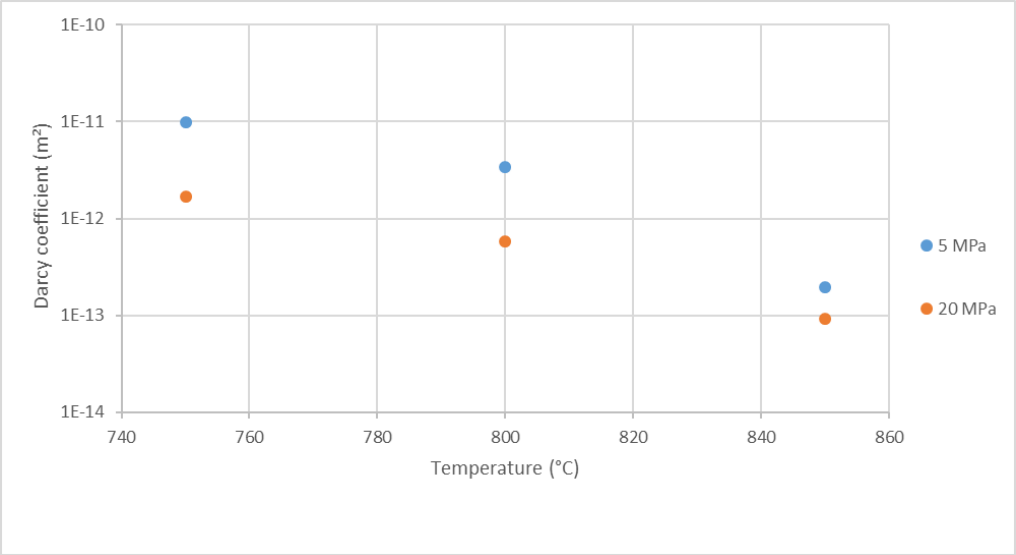

Figure 8 : Evolution of the Darcy coefficient depending on sintering parameters

It is quite clear from Figure 8 and

Sample	T1P1	T1P2	T2P1	T2P2	T3P1	T3P2
Darcy coefficient [m²]	9.12E-14	1.96E-13	5.74E-13	3.39E-12	1.69E-12	9.82E-12

Table 3 that pressure and most importantly temperature of the sintering process have a great influence on samples permeability. One should notice that the ordinate axis is in logarithmic scale. This means that, everything else being equal, it is possible to multiply permeability by almost 10 only by changing the sintering temperature by 50°C.

c) Computerized tomography scans and porosity rate

Now that the pressure losses were studied, it is interesting to relate it to the internal porous network structure.

As this network is a fully 3D structure, microscopic views of slices are not relevant to describe it. This is why computerised tomography scans (CT scans) of the samples has been made. CT scans work the same way as medical scanners. Thanks to multiple radiographies of a sample, it is possible to reconstruct its internal structure based on X rays absorption. This technique gives a 3D picture made of voxels (3D pixels) in greyscale. To have a usable picture, voxel size needs to be at least an order of magnitude lower than porosities. Otherwise, the porous network would be too much pixelated. This restricts the size of samples.

Then, the picture is made binary by manual thresholding. This means that the voxels will be split into two classes depending on their greyscale, thus clearly dissociating material (represented as black voxels) from porosities (white voxels). At this step, it is already possible to access the porosity ratio dividing the number of white voxels by the total one. It is also possible to dissociate the percolating porous network from closed porosities, which are not involved in the airflow, using region labelisation. The following computations will be conducted on the percolating porous network only.

Up to now, only T1P1 sample has been scanned yet. The sample was 10mm long, 6mm wide and 3.7mm thick, which is representative as the powder particles are much smaller. The resolution was satisfying as the voxels were cubes of 6.5µm side. After binarization, it has been found that the total porosity rate was 14.45%. The percolating porosity rate was 14.14% and the closed porosity rate 0.31%. Having a porous network mainly made of a single percolating one is a good thing, because it means that almost all porosities made in the manufacturing process are useful for the suction application. The low closed porosity rate 0.31% can be related to two causes. First, some powder particles might be hollow due to gas entrapment. Second, some tomography artefacts might have been interpreted as porosities after binarization.

The other samples should be scanned soon to be able to compare them with each other.

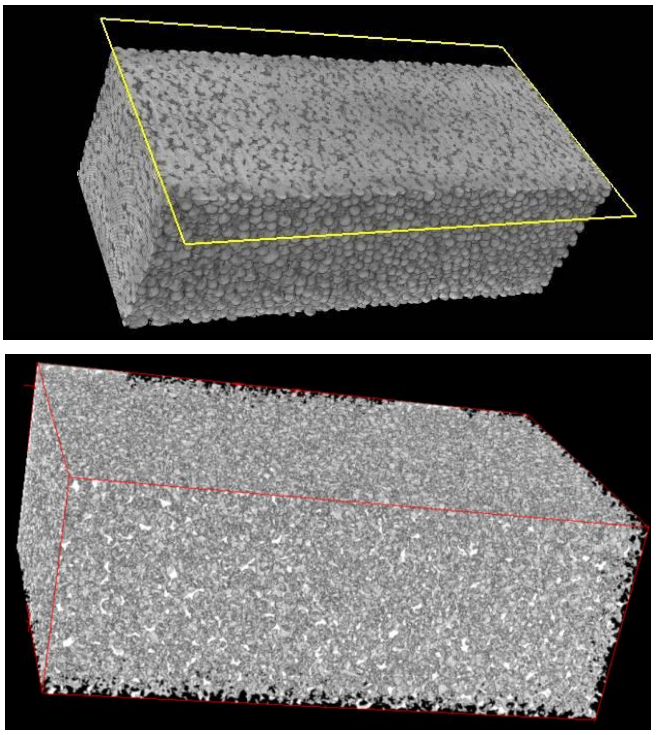

Figure 9 : CT scan of T1P1 sample (top) and its extracted porous network (bottom)

d) Tortuosity Evaluation

Tortuosity is an important parameter to describe percolating porous media, but its definition is still vague depending on the way it is measured. Here, it should describe how sinuous the path taken by the percolating flow inside a porous media is. As described in [8] tortuosity can be computed with geometric considerations or using physical phenomena. The choice made here is to use an open source Python package called Pytrax [9]. This package is easy to use and does not require too much computation resources. It is a diffusion-based model as it uses random walk of particles inside the porous network. At each time step, each particle has the same probability to jump to an available neighbour voxel using a 6-connectivity rule. Then, by comparing the axial square displacement inside the porous network in each direction to the one in free space, the tortuosity of the porous network can be computed in each direction. This approach enables to determine whether the porous network is isotropic or not. Indeed, with an anisotropic media, tortuosity in each direction should not be equal. Such a characteristic is desirable for the suction panel, as airflow should go through it easily without traveling too much in its length.

A first tortuosity computation has been conducted on the CT-scan of the T1P1 sample with 3E6 particles during 3E4 time steps.

Axis	**X (Thickness)**	**Y (Length)**	**Z (Width)**
Axial Tortuosity	6.08	9.65	10.5

Table 4: Tortuosity evaluation with Pytrax

The results in

Table 4 tend to confirm that the porous network is anisotropic as the tortuosity in X direction is significantly lower than in other directions. This direction is also the application direction of current and pressure in the manufacturing process.

This result should be confirmed with the evaluation of other samples CT scans soon.

5. Conclusion and Outlook

Partial powder densification by spark plasma sintering can give porous metallic materials suitable for suction applications. Moreover, permeability experiments showed that the manufacturing parameters had great impact on the suction performance. Besides, polishing proved to give an acceptable surface quality, but it needs to be fine enough to keep porosities open. Nevertheless, despite it worked correctly on the small samples used here, it will need to be adapted for larger panels. Finally, image analysis on CT scans seems to be a promising technique. Indeed, with appropriate programs, it is possible to compute many parameters that describe the geometry of the

internal porous network on a representative equivalent volume. Here, interesting results were obtained for porosity ratio and most importantly tortuosity. Indeed, the first results tend to confirm that tortuosity is lower in the direction of application of pressure and electric current. In the near future, pore size distribution will be studied.

When all the characterisation process will be mastered, it will be possible to use it on many different porous materials such as porous Ti-64 obtained by SPS with steel space holders or on samples made by LPBF.

6. References

[1] M. Kingsley-Jones, “FARNBOROUGH: Aero secrets of Boeing’s new Dreamliner,” *Flight Global*, Jul. 18, 2014. https://www.flightglobal.com/farnborough-aero-secrets-of-boeings-new-dreamliner/113955.article (accessed Nov. 10, 2021).

[2] B. Egreteau *et al.*, “Control of laminar turbulent transition using wall suction through a porous metal foam,” in *56th 3AF International Conference on Applied Aerodynamics*, Toulouse, Mar. 2022, p. 8.

[3] T. Nakamoto *et al.*, “Synthesis of Porous Titanium with Directional Pores by Selective Laser Melting,” *Int. J. Automation Technol.*, vol. 6, no. 5, pp. 597–603, Sep. 2012, doi: 10.20965/ijat.2012.p0597.

[4] D. I. Yushin, A. V. Smirnov, N. W. Solis Pinargote, P. Y. Peretyagin, and R. Torrecillas San Millan, “Modeling Process of Spark Plasma Sintering of Powder Materials by Finite Element Method,” *Materials Science Forum*, vol. 834, pp. 41–50, 2015, doi: 10.4028/www.scientific.net/MSF.834.41.

[5] D. Dudina, B. Bokhonov, and E. Olevsky, “Fabrication of Porous Materials by Spark Plasma Sintering: A Review,” *Materials*, vol. 12, no. 3, p. 541, Feb. 2019, doi: 10.3390/ma12030541.

[6] R. Yamanoglu, N. Gulsoy, E. Olevsky, and H. O. Gulsoy, “Production of porous Ti5Al2.5Fe alloy via pressureless spark plasma sintering,” *Journal of Alloys and Compounds*, vol. 680, pp. 654–658, Sep. 2016, doi: 10.1016/j.jallcom.2016.04.176.

[7] Jeanne Methel, “An Experimental Investigation of the Effects of Surface Defects on the Laminar-Turbulent Transition of a Boundary Layer with Wall Suction,” Ph.D thesis, ISAE-Supaéro, Université de Toulouse, 2019.

[8] J. Fu, H. R. Thomas, and C. Li, “Tortuosity of porous media: Image analysis and physical simulation,” *Earth-Science Reviews*, vol. 212, p. 103439, Jan. 2021, doi: 10.1016/j.earscirev.2020.103439.

[9] T. G. Tranter, M. D. R. Kok, M. Lam, and J. T. Gostick, “pytrax: A simple and efficient random walk implementation for calculating the directional tortuosity of images,” *SoftwareX*, vol. 10, p. 100277, Jul. 2019, doi: 10.1016/j.softx.2019.100277.